Supplementary Information

Bone marrow resident antigen presenting cells promote peripheral tolerance by inducing autoreactive regulatory T cells

Chih-Yeh Chen[1,2,16,†], Felix Klug[2,16,‖], Siao-Han Wong[3,4], Franziska Sanna[1,‡], Sheena Pinto[5,¶], Alexander Wurzel[1], Tomoyoshi Yamano[6,§], Dania Riegel[1,a], Michael Delacher[1,7,b,c], Maria Dinkelacker[3,4,d], Charles D. Imbusch[3,4,b], Abdelrahman Mahmoud[3,4,e], Roman Kurilov[3,f], Miodrag Gužvić[8,g], Claudia Gebhard[1,9], Guido Wabnitz[10], Valentina Volpin[1,2,h], Ayse Nur Menevse[1,2], Yvonne Samstag[10], Pärt Peterson[11], Michael Rehli[1,9], Slava Stamova[1,2], Maria Xydia[1,2], Christoph A. Klein[8,12], Mark S. Anderson[13], Christian Schmidl[1], Markus Feuerer[1,7], Benedikt Brors[3,14,15], Philipp Beckhove[1,2]

Supplementary Figures

Figure S1

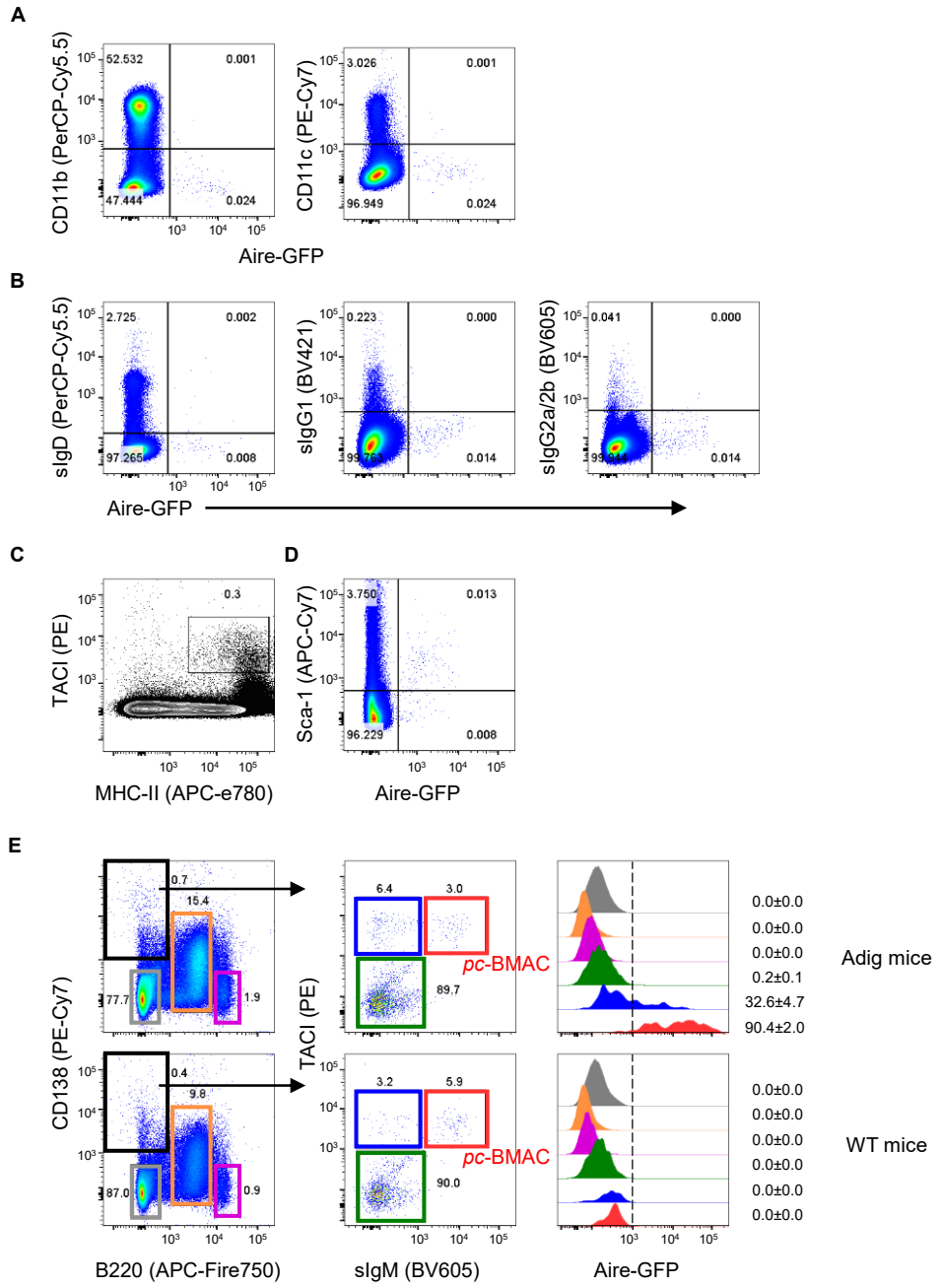

Figure S1. Related to Figure 2. Characterization of BM Aire-GFP$^+$ cells in Adig mice.

(A and B) Flow cytometric analysis of expression of surface markers and isotypes of immunoglobulin. Frequencies of each quadrant among total BM cells are depicted in percentage. **(C)** Gating strategy of MHC-II+TACI+ cells. Number indicates percentage of gated cells among total BM cells. **(D)** Flow cytometric analysis of Sca-1 expression. Frequencies of each quadrant among total BM cells are depicted in percentage. **(E)** Gating strategy of *pc*-BMACs in Adig and WT mice. Frequencies of Aire-GFP$^+$ cells among each population are depicted in percentage (mean ± SEM). Data are representative of two independent experiments (n ≥ 3).

Figure S2

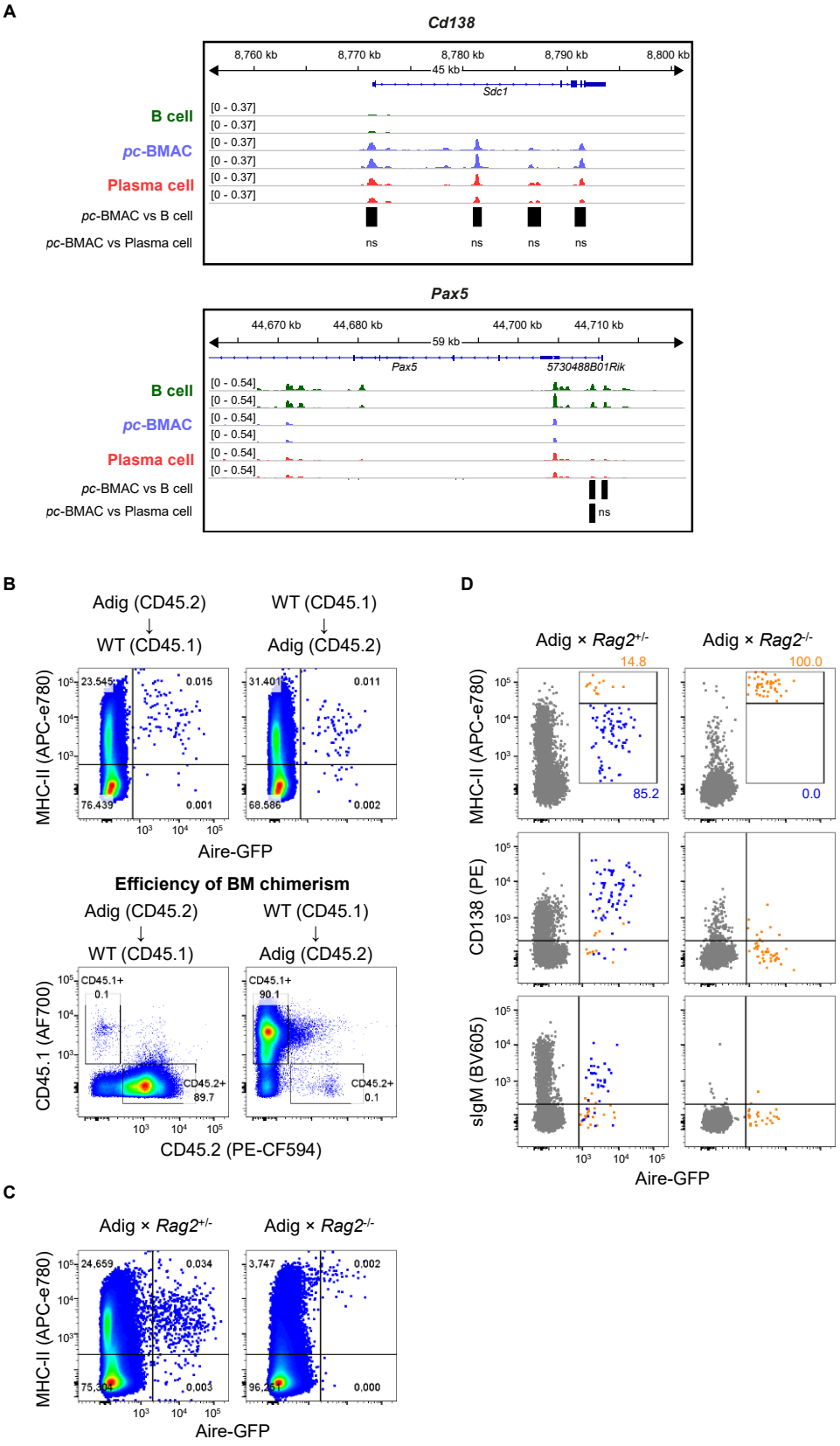

Figure S2. Related to Figure 2. Plasma cell features of *pc*-BMACs.

(A) Chromatin accessibility of *Sdc1* and *Pax5* loci in *pc*-BMACs, B cells (CD138^{-}B220^{hi}) and plasma cells (CD138^{+}TACI^{+}B220^{-}) in the BM. Gene information and genomic location is shown on top. All

samples are group-normalized to allow peak height comparison (scale of ATAC-seq signal shown in brackets). Bars below represent significant peaks between the compared groups. **(B)** Representative data of Aire-GFP^{+}MHC-II^{+} cells (top) and CD45.1 or CD45.2 single positive cells (bottom) among total BM mononuclear cells (MNCs) of reciprocal BM chimeras: Adig→WT and WT→Adig (n = 4). **(C)** Representative data of Aire-GFP^{+}MHC-II^{+} cells among total BM MNCs of RAG2$^{+/-}$ and RAG2$^{-/-}$ Adig mice.

Figure S3

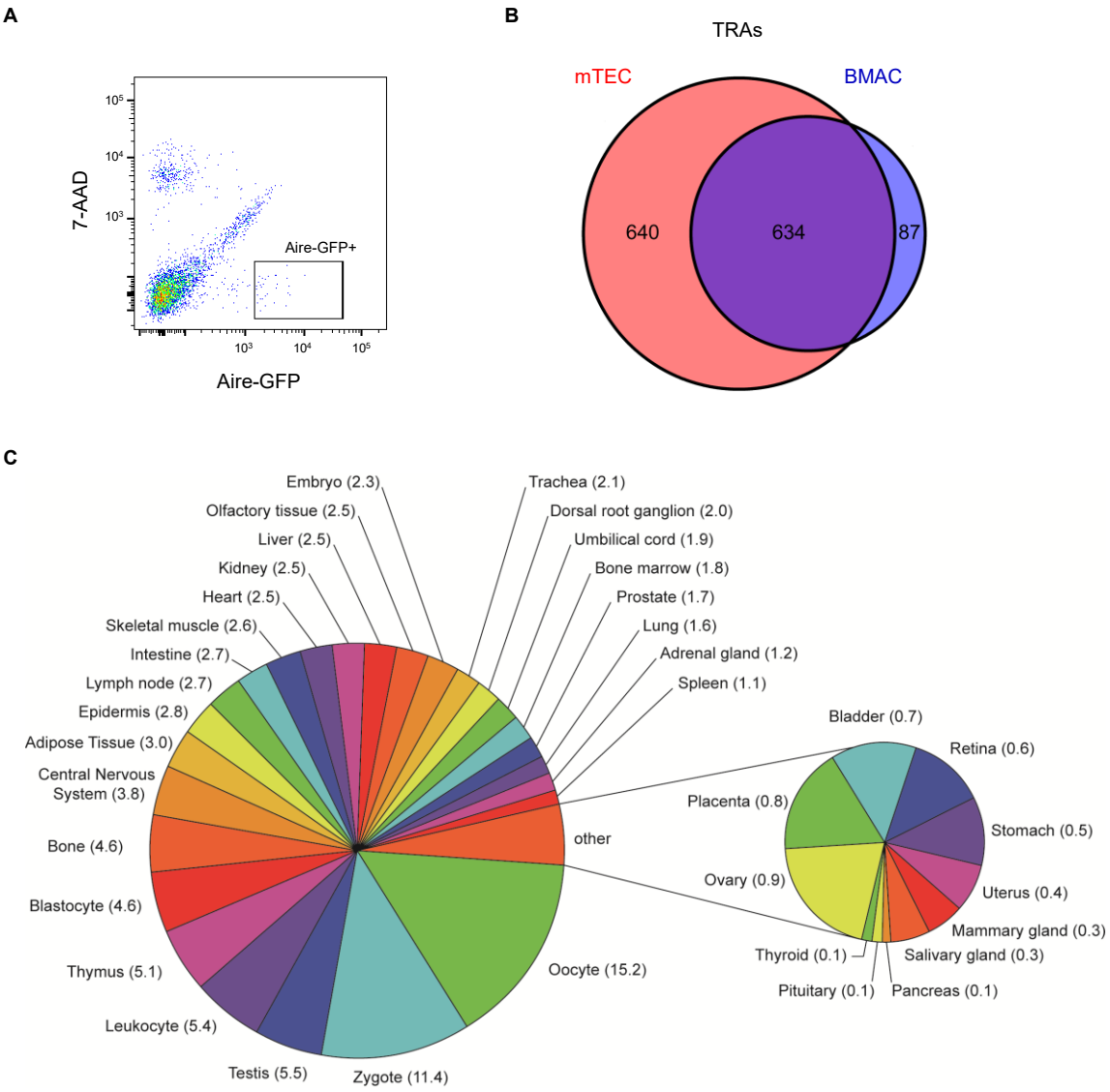

Figure S3. Related to Figure 3. Promiscuous gene expression in BMACs.

(A) Sorting strategy of BMACs from Adig mice for gene expression microarray. **(B)** Venn diagram of the numbers of TRA genes expressed exclusively in either mTECs or BMACs, or commonly expressed in both. **(C)** Distribution of the tissue types represented by the TRAs expressed by BMACs. Numbers in bracelets indicate percentages of each tissue type.

Figure S4

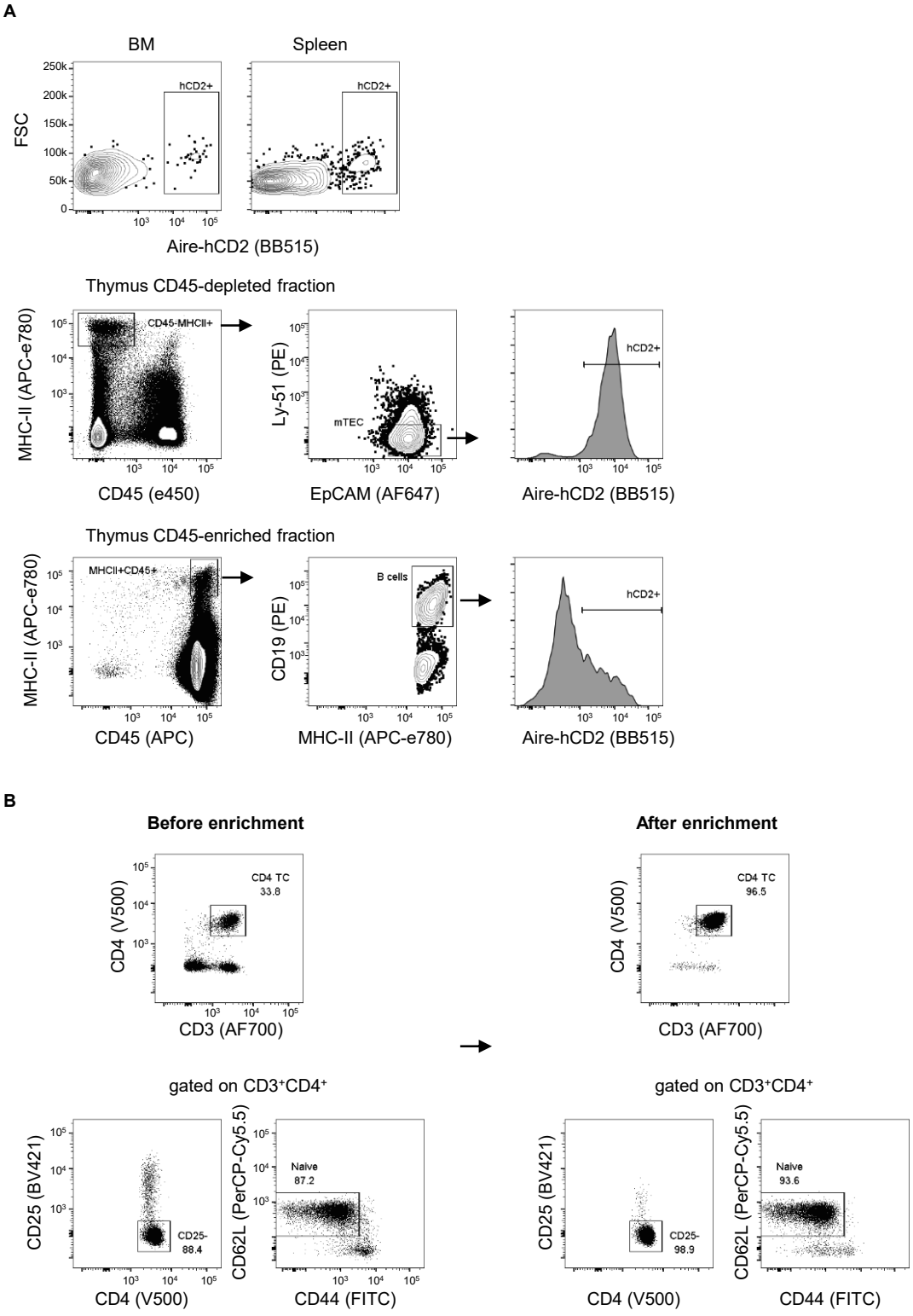

Figure S4. Related to Figure 4. Isolation of Aire-expressing APCs and naïve CD4$^+$ T cells for antigen presentation assays.

(A) Sorting strategies of Aire-expressing APCs from BM, spleen, and thymus of Aire-HCO mice. **(B)** Representative data of isolation of naïve CD4$^+$ T cells from spleens of WT Balb/c mice by magnet-activated enrichment (negative selection).

Figure S5

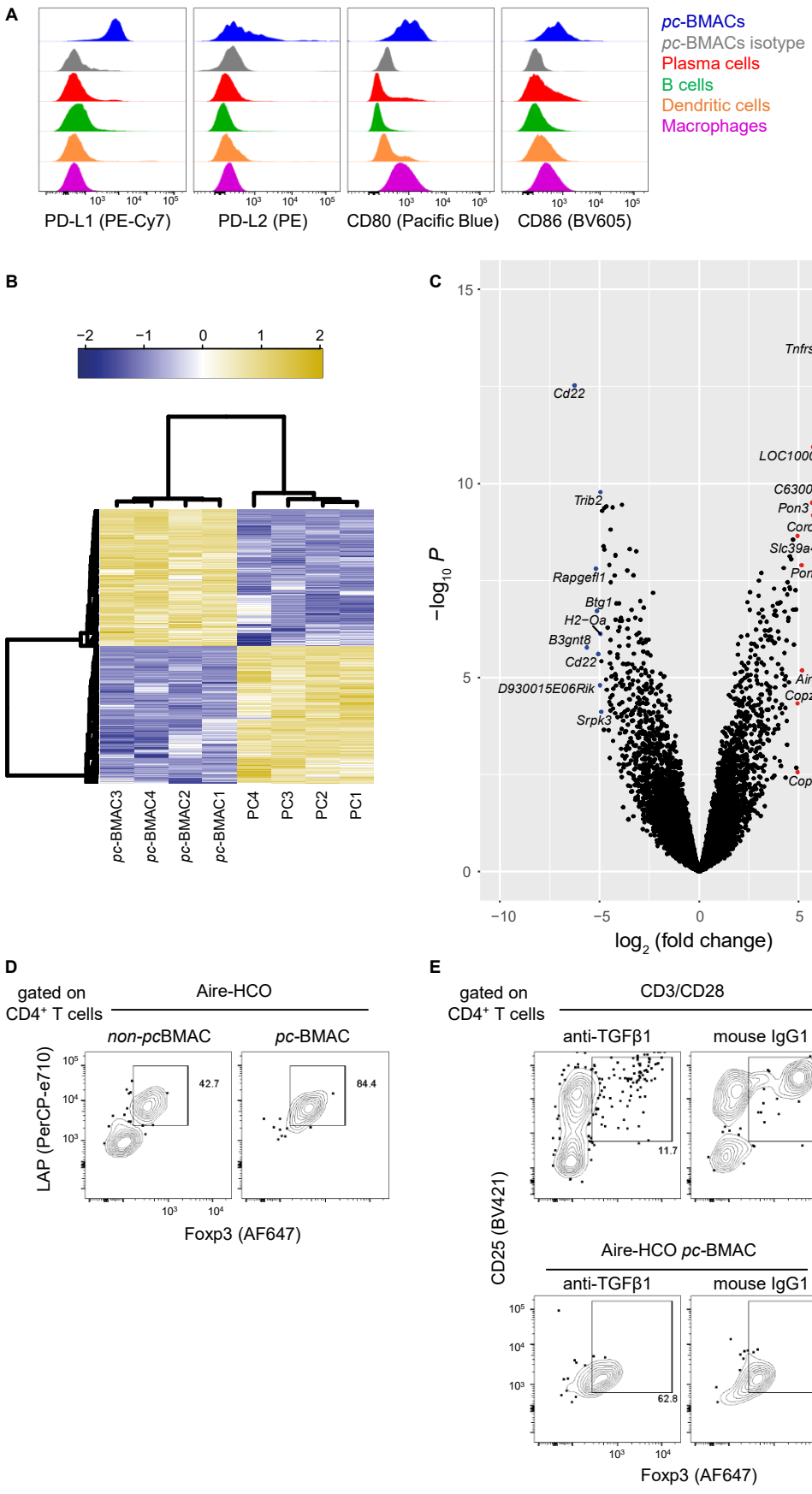
A
pc-BMACs
pc-BMACs isotype
Plasma cells
B cells
Dendritic cells
Macrophages
PD-L1 (PE-Cy7)
PD-L2 (PE)
CD80 (Pacific Blue)
CD86 (BV605)
B
pc-BMAC3
pc-BMAC4
pc-BMAC2
pc-BMAC1
PC4
PC3
PC2
PC1
C
Ly6a
Tnfrsf17
Chst1
Cd22
LOC100043986
C630004H02Rik
Trib2
Pon3
G6pc2
Coro2b
Slc39a4
Rapgef1
Pon3
Btg1
H2−Qa
B3gnt8
Cd22
Aire
D930015E06Rik
Copz2
Srpk3
Copz2
−log10 P
log2 (fold change)
D
gated on CD4+ T cells
Aire-HCO
non-pcBMAC
pc-BMAC
LAP (PerCP-e710)
42.7
84.4
Foxp3 (AF647)
E
gated on CD4+ T cells
CD3/CD28
anti-TGFβ1
mouse IgG1
11.7
36.8
Aire-HCO pc-BMAC
anti-TGFβ1
mouse IgG1
62.8
60.4
CD25 (BV421)
Foxp3 (AF647)

Figure S5. Related to Figure 5. *pc*-BMACs induce Treg conversion *in vitro*.

(A) Flow cytometric analysis of CD80, CD86, PD-L1 and PD-L2 expression on Aire-GFP$^+$CD138$^+$B220$^-$ *pc*-BMACs and various APC subsets (CD138$^+$B220$^-$ plasma cells, CD138$^-$B220^{hi} B cells, CD11c$^+$ DCs, F4/80$^+$ macrophages) from the BM of Adig mice (n = 3). **(B)** Heatmap of differentially expressed genes (adjusted $P < 0.05$) in *pc*-BMACs compared to BM plasma cells (PC). **(C)** Volcano plot of genes analyzed (*pc*-BMAC vs PC), with labels of the genes which had a significant fold change > 30 (red) or < -30 (blue). **(D)** Frequencies of LAP$^+$Foxp3$^+$ cells among HA-specific CD4$^+$ cells after co-culture with non-*pc*BMACs or *pc*-BMACs from Aire-HCO mice. **(E)** Frequencies of CD25$^+$Foxp3$^+$ cells among HA-specific CD4$^+$ cells after co-culture with CD3/CD28 activation beads, non-*pc*BMACs or *pc*-BMACs from Aire-HCO mice in the presence of anti- TGFβ1 antibody (clone 19D8) or mouse IgG1 isotype control antibody.

Figure S6

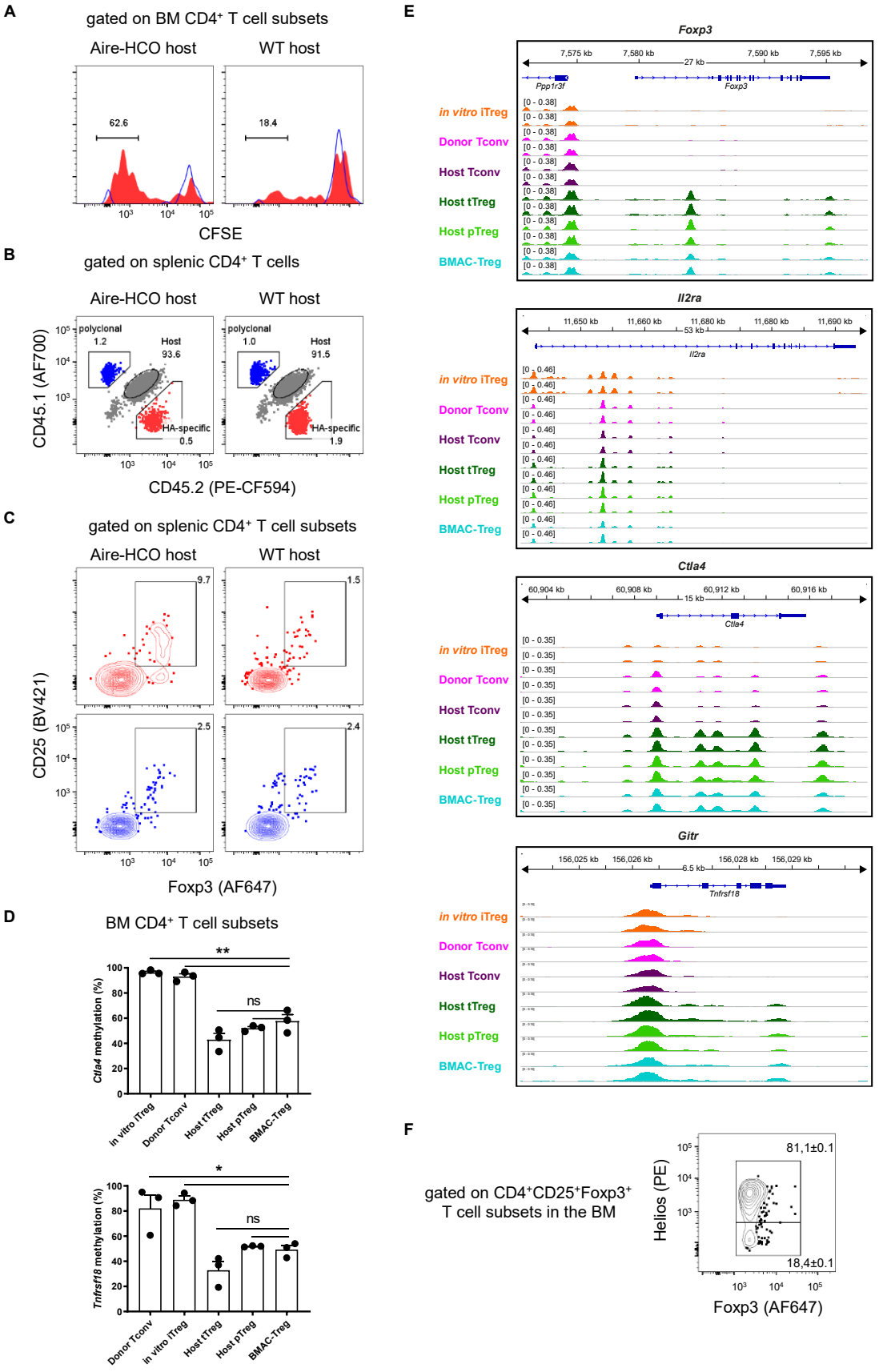

Figure S6. Related to Figure 6. HA-specific T cells are activated and converted to stable Tregs in the BM.

(A) Proliferation of $CD45.2^+$ HA-specific $CD4^+$ T cells (red) and $CD45.1^+$ polyclonal $CD4^+$ T cells (blue) in the BM of $CD45.1^+CD45.2^+$ hosts on day 3 post-transfer (n = 4). Numbers indicate percentages of gated cells among HA-specific donor $CD4^+$ T cells. **(B)** Proportions of $CD45.2^+$ HA-specific $CD4^+$ T cells (red) and $CD45.1^+$ polyclonal $CD4^+$ T cells (blue) in the spleen of $CD45.1^+CD45.2^+$ hosts on day 14 post-transfer (n = 4). Numbers indicate percentages of gated cells among $CD4^+$ T cells. **(C)** Frequencies of $CD25^+Foxp3^+$ Treg cells of $CD45.2^+$ HA-specific $CD4^+$ T cells (red) and $CD45.1^+$ polyclonal $CD4^+$ T cells (blue) in the spleen of $CD45.1^+CD45.2^+$ host on day 14 post-transfer (n = 4). Numbers indicate percentages of gated cells. **(D)** CG methylation status of *Ctla4* and *Tnfrsf18* loci in BMAC-Tregs, Donor Tconvs, Host tTregs and Host pTregs from BM $CD4^+$ T cells, as well as *in vitro* iTregs (n = 3, mean ± SEM). **(E)** Chromatin accessibility of *Foxp3, Ilr2a, Ctla4,* and *Gitr* loci in BMAC-Tregs, Donor Tconvs, Host tTregs, Host pTregs, and Host Tconvs from BM $CD4^+$ T cells, as well as *in vitro* iTregs. Gene information and genomic location is shown on top. All samples are group-normalized to allow peak height comparison (scale of ATAC-seq signal shown in brackets). **(F)** Frequencies of tTregs ($Helios^+Foxp3^+$) and pTregs ($Helios^-Foxp3^+$) among $CD25^+Foxp3^+$ Treg cells in the BM, shown in percentage (n = 3, mean±SEM). $P > 0.05$; *, $P < 0.05$; **, $P < 0.01$. Data are representative of three (**A-C**) or two (**D-F**) independent experiments.

Figure S7

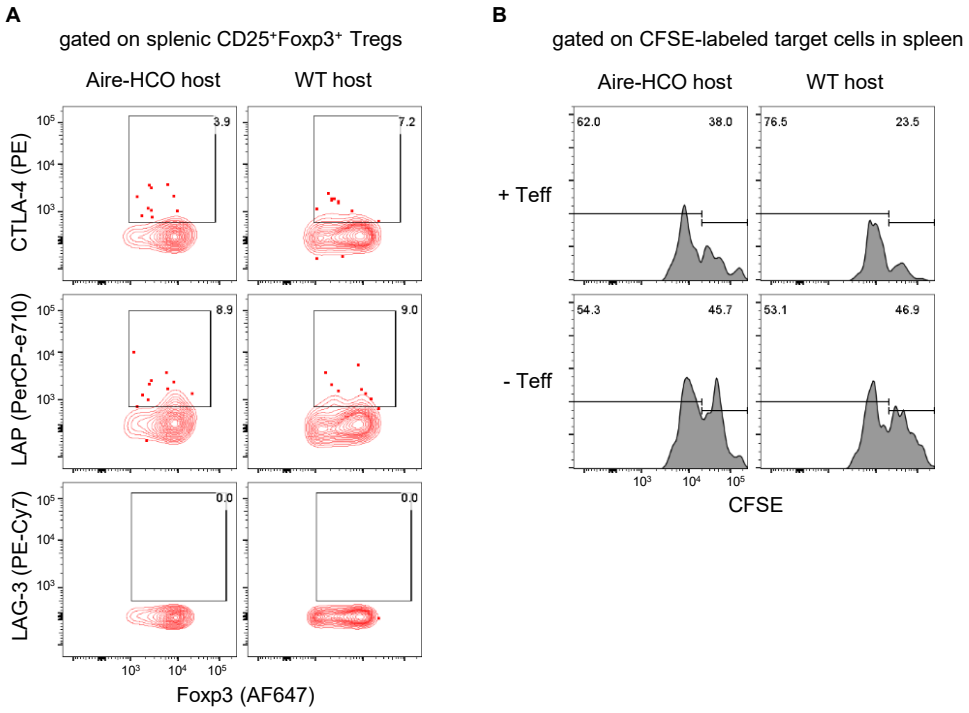

Figure S7. Related to Figure 7. HA-specific Tregs induced in the spleen manifest no activated status and suppressive function.

(A) Representative data of the frequencies of CTLA-4$^+$, LAP$^+$ and LAG-3$^+$ cells among CD25$^+$Foxp3$^+$ HA-specific Treg cells in the spleen of Aire-HCO or WT hosts (n = 4). Numbers indicate percentages of gated cells. **(B)** Frequencies of B220$^+$CFSE^{high} and B220$^+$CFSE^{low} target cells and specific cytotoxicity (18 h after target cell transfer) in the spleen of Aire-HCO or WT hosts with or without co-transfer of HA-specific effector T cells. Numbers in histograms indicate percentages of gated B220$^+$ cells (n = 3). Data are representative of three (**A**) or two (**B**) independent experiments.

Supplementary Tables

Table S1. Related to Figure 3. TRAs expressed in BMACs.

TRA genes expressed (detection $P < 0.01$) in BMACs. TRA genes exclusively expressed in BMACs but not in mTECs are highlighted in yellow. Self-antigens associated with autoimmune diseases are labeled in red. Tumor-associated antigens are labeled in blue.

Table S2. Related to Figure 3. Aire-regulated genes in *pc*-BMACs.

Differentially expressed genes in $CD138^{+}B220^{-}TACI^{+}$Aire-$GFP^{+}$ $Aire^{+/+}$ *pc*-BMACs compared to $CD138^{+}B220^{-}TACI^{+}IgM^{+}$ $Aire^{-/-}$ *pc*-BMACs. Genes classified as TRAs are highlighted in yellow.